T.R.
GEBZE TECHNICAL UNIVERSITY
GRADUATE SCHOOL OF NATURAL AND APPLIED SCIENCES

VHF CHANNEL MODELING FOR WIRELESS SENSOR NETWORKS

AİZAT AİTALİEVA
A THESIS SUBMITTED FOR THE DEGREE OF
MASTER OF SCIENCE
DEPARTMENT OF ELECTRONIC ENGINEERING

GEBZE
2015

T.R.

GEBZE TECHNICAL UNIVERSITY

GRADUATE SCHOOL OF NATURAL AND APPLIED SCIENCES

VHF CHANNEL MODELING FOR WIRELESS SENSOR NETWORKS

AİZAT AİTALİEVA

A THESIS SUBMITTED FOR THE DEGREE OF

MASTER OF SCIENCE

DEPARTMENT OF ELECTRONIC ENGINEERING

THESIS SUPERVISOR

ASSOC. PROF. DR. HASARİ ÇELEBİ

GEBZE

2015

T.C.
GEBZE TEKNİK ÜNİVERSİTESİ
FEN BİLİMLERİ ENSTİTÜSÜ

KABLOSUZ DUYARGA AĞLARI İÇİN VHF KANAL MODELLEME

AİZAT AİTALİEVA
YÜKSEK LİSANS TEZİ
ELEKTRONİK MÜHENDİSLİĞİ ANABİLİM DALI

DANIŞMANI
DOÇ. DR. HASARİ ÇELEBİ

GEBZE
2015

GEBZE TEKNİK ÜNİVERSİTESİ	**YÜKSEK LİSANS JÜRİ ONAY FORMU**

GTÜ Fen Bilimleri Enstitüsü Yönetim Kurulu'nun 29/06/2015 tarih ve 2015/41 sayılı kararıyla oluşturulan jüri tarafından 09/07/2015 tarihinde tez savunma sınavı yapılan Aizat AİTALİEVA'nın tez çalışması Elektronik Mühendisliği Anabilim Dalında YÜKSEK LİSANS tezi olarak kabul edilmiştir.

JÜRİ

ÜYE
(TEZ DANIŞMANI) : Doç. Dr. Hasari ÇELEBİ

ÜYE : Prof. Dr. Murat UYSAL

ÜYE : Yrd.Doç.Dr.Köksal HOCAOĞLU

ONAY

Gebze Teknik Üniversitesi Fen Bilimleri Enstitüsü Yönetim Kurulu'nun

...../...../.....tarih ve ...../..... sayılı kararı.

İMZA/MÜHÜR

SUMMARY

Nowadays, wireless communication systems have become an essential part of life. To improve its performance and bandwidth efficiency the characteristics of the operating wireless channel must be well known. This can be achieved by sounding, estimation, and modeling of the wireless channel. In this work, the propagation channel for Wireless Sensor Network Systems, which are operated at 145 MHz Very High Frequency (VHF) communication band, is modeled with simulations and empirical measurements. The simulations are performed by using electromagnetic ray-tracing based simulation software, i.e. Wireless InSite. On the other hand, the empirical measurement is performed in the real environment. Both measurements are carried out in hilly and irregular terrain in Beypazarı-Ankara İnözü valley. Such terrain is selected as the measurement environment due to its dense hilly characteristics. The large-scale and small-scale statistical parameters of the channel are obtained for both empirical and ray-tracing based measurements. After, comparison and discussion of these results are performed. The channel characteristics are obtained in order to use to model the profile that can help to develop communication system for monitoring applications such as border security, surveillance of petrol/gas pipes or critical infrastructure/field in hilly and irregular regions.

Keywords: Channel modeling; Ray-tracing; Small-scale fading; Large-scale fading.

ÖZET

Kablosuz haberleşme sistemleri son yıllarda hayatımızın her alanında çokça yer almaya başlamıştır. Kablosuz haberleşme sistemlerinin performansını ve bant genişliği verimliliğini arttırmak için haberleşmenin gerçekleştirileceği kablosuz kanal ortamının iyi bilinmesi gerekmektedir. Bu işlem kanalı dinleme, kestirim ve modelleme ile gerçekleştirebilir. Bu çalışmada Kablosuz Duyarga Ağ Telemetre sistemleri için 145 MHz VHF haberleşme bandında simülasyon ve ampirik ölçümler yaparak kanal modellenmesi gerçekleştirilmiştir. Simülasyon ölçümleri Wireless InSite elektromanyetik yayılım ışın izleme tabanlı kanal modelleme benzetim yazılımı ile gerçeklenmiştir. Ampirik ölçümleri ise gerçek saha ortamda yapılmıştır. Ölçüm ortamı olarak Ankara'nın Beypazarı ilçesi İnözü vadisi seçilmiştir. Ölçüm için o ortamın seçilmesinin nedeni yoğun kayalık/dağlık özelliğe sahip olmasıdır. Kanalın büyük ölçekli ve küçük ölçekli istatistiksel parametreleri hem ampirik ve ışın izleme tabanlı ölçümler için elde edilmiştir ve birbiri ile karşılaştırmıştır. Elde edilen kanal karakteristikleri tepelik ve düzgün olmayan bölgelerde kullanılabilecek izleme uygulamaları, sınır güvenliği, benzin/gaz boruları gözetim veya kritik altyapılı alanlarda kullanılan haberleşme sistemleri geliştirilmesinde katkı sağlayacaktır.

Anahtar Kelimeler: Kanal modelleme; Işın izleme; Büyük-Ölçekli Sönümleme; Küçük-Ölçekli Sönümleme.

ACKNOWLEDGEMENTS

This work is supported by the Ministry of Science, Industry and Technology of Turkey and by ASELSAN Inc. under Grant SANTEZ 01553.STZ.2012-2. I would like to express my gratitude to both institutions for their support.

I would like to express my deepest and sincere gratitude to my thesis advisor, Dr. Hasari Çelebi, without his continuous support, encouragement and constructive criticism, it may have been impossible for me to complete this thesis.

I would like to sincerely thank Dr. Murat Uysal for his support throughout this project.

I also thank the research assistant Gökhan Çelik for his assistance and most valuable supports, who willingly sacrificed his time to read my drafts and gave me invaluable and stimulating advice.

Finally yet importantly, for supporting me in any situation, and with all their efforts, my family deserves my deepest gratitude.

TABLE of CONTENTS

LIST of ABBREVIATIONS and ACRONYMS

Acronyms and Abbreviations		Descriptions
ARB	:	Arbitrary Waveform Generator
CIR	:	Channel Impulse Response
CTF	:	Cannel Transfer Function
EM	:	Electromagnetic
FFT	:	Fast Fourier Transfer
I/Q	:	In-phase and Quadrature
LOS	:	Line-of-sight
MHz	:	Mega Hertz
NLOS	:	Non-line-of-sight
PAPR	:	Peak to Average Power Ratio
PDP	:	Power Delay Profile
RMS	:	Root Mean Square
RX	:	Receiver
TX	:	Transmitter
VHF	:	Very High Frequency
WI	:	Wireless InSite

LIST of FIGURES

LIST of TABLES

1. INTRODUCTION

Today, wireless communication systems have become an essential part of daily life [1]. The radio channel between transmitter (TX) and receiver (RX) is the transmission medium for wireless communication systems. Due to physical phenomena like reflection, diffraction, and scattering the wireless signal that is traversed the path from a TX to a RX faces distortion or impairs in various ways [2], [3]. When a propagated electromagnetic wave incident onto an interacting object with smooth, very large dimension compared to the signal wavelength the reflection of the signal occurs. This makes the transmitted signal power to be reflected back. Diffraction of the signal occurs when the obstacle on the path has a surface with sharp irregular or small openings which spread out the electromagnetic wave. If the transmitted signal is deviated from a straight path by one or more local obstacles which have a small dimension compared to the electromagnetic wave's wavelength than the scattering of the signal occurs. As the result of these physical phenomena, the transmitted signal can get to the RX via a number of propagation paths. The different multipath components (MPCs) can have different phases and when they are added at the RX side they constructively or destructively interfere with each other. The phases of the MPCs depend on the position of the TX, the RX and the signal interacting objects, and the amplitude of the total signal changes with time when either of them is moving short distances. This effect is called small scale fading. If the TX and/or the RX move(s) through a large distance large scale fading occurs. It is caused by path loss of the signal as a function of distance and shadowing by large objects. So this means that the signal propagation manner over wireless channel varies within environment, and the aim of the channel modeling lies on understanding it. The detailed information about the channel helps to improve performance and bandwidth efficiency of the wireless communication systems [4], [5]. This can be achieved by sounding, estimation, and modeling wireless channel [6], [7].

The motivation of this work is to model the wireless propagation channel for Wireless Sensor Network Systems which operate at 145 MHz Very High Frequency (VHF) communication band. The wireless propagation channel is modeled with simulations and empirical measurements for hilly and irregular terrain. At the VHF

frequency band propagation of electromagnetic waves take place in the troposphere, and communication occurs through the direct and ground reflected components of the transmitted signal [3], [8].

The simulations are performed by using electromagnetic ray-tracing based simulation software, i.e. Wireless InSite [9], [10]. The empirical measurement is performed in the real environment. For channel sounding, the Rohde-Schwarz signal generator SMBV100A is used as the TX, whereas Rohde-Schwarz signal and spectrum analyzer FSV7 is used as the RX [11], [12]. Both measurements are carried out in hilly and irregular terrain in Beypazarı-Ankara İnözü valley. Figure 1.1 illustrates the satellite image of the measurement region.

Figure 1.1: The satellite image of the measurement region (Google Earth).

Such terrain is selected as the measurement environment due to its dense hilly characteristics. The reason of selecting this profile is the fact that this model can help

to develop border security applications, surveillance of petrol/gas pipes or critical infrastructure/field in hilly and irregular regions.

By analyzing obtained data from measurement, the large-scale and small-scale statistical characteristics of the channel are obtained for both empirical and ray-tracing based measurements and compared with each other.

2. RELATED WORKS

Previous studies of VHF frequency band channel modeling have been carried out for ground to ground, ground to plane, plane to plane etc. in different parts of the VHF band with fixed and mobile terminals. Studies aimed to address the ground to ground channel modeling at VHF band are mostly done for urban as well as in rural and forested environments [13], [14], [15], [16], [17],[18]. However, to the best of our knowledge, very few publications are available in the literature that discuss the issue of channel modeling at the VHF band in hilly, irregular terrain with fixed terminals. For instance, VHF propagation measurement at a frequency of 110.6 MHz at low altitude over hilly, forested terrain have been performed to develop a computer-based propagation model which could predict path loss by giving the terrain profile between the transmitter and receiver [13]. But, propagation of wave in the hilly, forested area faces different propagation mechanisms than only hilly terrain. Additionally, taking measurement at different altitude changes propagation manner of signal. As another example can be given the measurement that have been carried out at 210 MHz frequency by Andreas Zogg in 1987 in the city and the outskirts of Bern which is one of the hilly regions of Switzerland, in order to find the multipath delay spread of terrains [8]. The measurement that held in outskirt of Bern can be considered as the closest work to ours. However, authors of paper reported that at measurement area there was one-family houses, and direct signal may attenuated by this obstacle. In our case, measurement region does not contain such obstacles. It is well known that even small changes in the topography or the morphology of the area can cause significant changes in the wave propagation and wrong prediction.

Related works in the field of real measurement and ray-tracing based channel modeling for urban, rural and suburban regions and indoor can be referred [19], [20], [21], [22] references. However, none of these studies coincide with our work geographically and in used frequency band. Additionally, no studies have done at 145 MHz frequency at hilly and irregular terrain yet. This study in modeling of profile for wireless sensor networks at VHF frequency band plays an important role in developing communication system for monitoring applications.

3. RAY-TRACING BASED CHANNEL MODELING

Ray-tracing based channel modeling at 145 MHz VHF communication band for hilly and irregular terrain is performed by Wireless Insite (WI) software package from Company Remcom. WI is electromagnetic modeling instrument for predicting the propagation of electromagnetic waves over defined environment. Using WI the physical characteristics of the terrain and building features can be modeled. According to this model electromagnetic calculation is performed. And then the signal propagation characteristics can be evaluated [9], [10].

The three dimensional Geographical Informational System-GIS data for measurement environment is provided by The GeoCommunity web site [23]. GIS data of Beypazarı-Ankara İnözü valley which has the desired geographic features is imported for ray-tracing based channel modeling. In Figure 3.1 is illustrated 3 dimensional (3D) measurement environments in Wireless InSite.

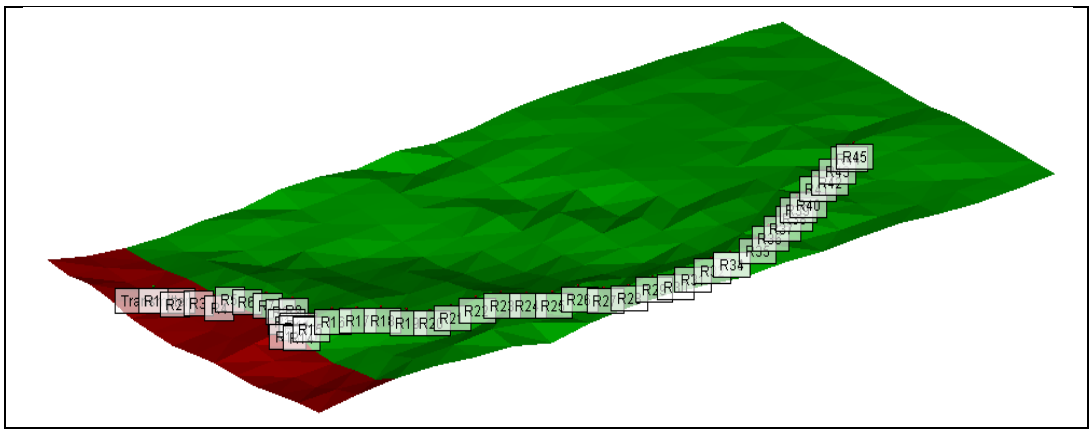

Figure 3.1: The measurement environment illustrated in Wireless InSite.

3.1. Measurement Setup

TX/RX locations are specified in the measurement environment using WI site-defining tools. It also can be imported from an external file. Selection of an entire set or an individual point of TX/RX is possible. In this study one TX and 45 individual points of RXs are used for ray-tracing based channel modeling. Defined TX and RXs point's locations can be seen in Figure 3.1. WI is the propagation software that uses

advanced ray-tracing techniques. It gives the user the opportunity to work with different models and model parameters. The model and related parameters used in our study are presented in Table 3.1.

Table 3.1: WI system parameters for ray-tracing Propagation channel.

Carrier frequency	145 MHz
Bandwidth	2 MHz
Output power of amplifier	50 Watt (47dBm)
Transmitted signal waveform	Raised Cosine
Propagation model	Vertical Model
Antenna Type	Omni-directional
Temperature	283(K)
Transmitter Antenna Height	4m
Transmitter/Receiver Antenna Gain	2.1 dBi
Receiver Sensitivity	-160 dBm

3.2. Data Collection

Data collection is realized by locating TX on the region's the highest place which is approximately 1590 m above sea level, and RXs along the route with the interval 500 m apart from each other along the measurement environment. The height profile of the RXs location points are shown in Figure 3.2. Additionally, the line-of-sight (LOS) distance between TX and RX can be found in Table 3.1. From this table it can be seen that distance between the TX and the RX does not increase in linear manner. The reason for this is curved feature of the route along RXs are located. Using this measurement environment and system parameters on WI program channel modeling statistics for each receiver location points have been evaluated and determined. Results are given in measurement results and discussion comparison of results chapter.

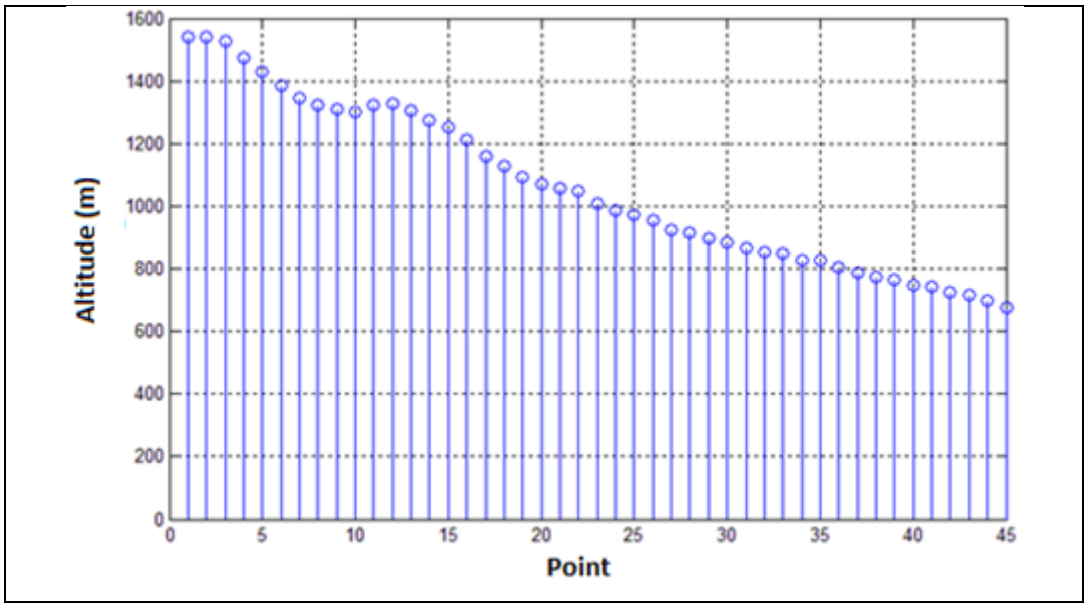

Figure 3.2: The height profile of receivers' location points.

Table 3.2: Distance between transmitter and receiver location points.

Point	Distance (km)	Point	Distance (km)	Point	Distance (km)
P1	0,508444	P16	4,439231	P31	10,91063
P2	0,902649	P17	4,849526	P32	11,28874
P3	1,422356	P18	5,329008	P33	11,50757
P4	1,517287	P19	5,789182	P34	11,8165
P5	1,903447	P20	6,101328	P35	12,09485
P6	2,347531	P21	6,534149	P36	12,37643
P7	2,725646	P22	6,968579	P37	12,68536
P8	2,955733	P23	7,460933	P38	12,83982
P9	3,032965	P24	7,938806	P39	13,13909
P10	3,390163	P25	8,410243	P40	13,45446
P11	3,444869	P26	8,933168	P41	13,81166
P12	3,549454	P27	9,388515	P42	14,0884
P13	3,898607	P28	9,837426	P43	14,43917
P14	3,763451	P29	10,25094	P44	14,60328
P15	4,008019	P30	10,56952	P45	14,62581

4. EMPIRICAL BASED CHANNEL MODELING

In this chapter, information about empirical based channel modeling measurement setup and signal design is provided, a link budget analysis is performed, and data collection is discussed.

4.1. Measurement Setup

Block diagram of measurement setup that is used in the field to model channel sounding system is given in Figure 4.1, and Table 4.1 shows list of equipment and their usages. As shown in the above measurement scheme, output of the signal generator is connected to the RF power amplifier (PA) device and PA's output is connected to the transmitter antenna. Signal that is propagated through wireless channel is captured by the receiver antenna and recorded for further analysis. Due to a long range measurement GPS clock source is used for time and frequency synchronization of TX and RX.

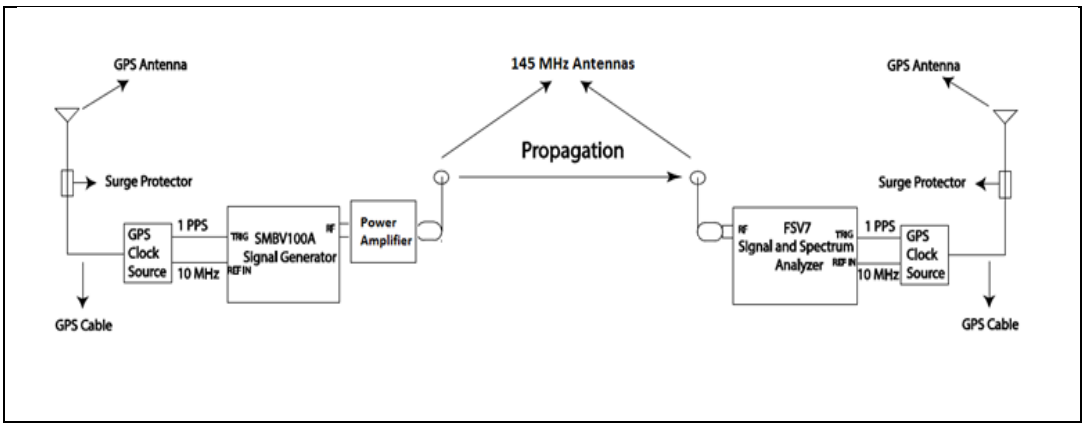

Figure 4.1: Block diagram of the measurement setup.

Rohde & Schwarz SMBV100A vector signal generator is used as a transmitter in the channel sounding process which offers excellent RF performance, high output level and short setting times with a wide frequency range from 9 kHz to 6 GHz. The signal generator offers various types of modulation techniques, as amplitude, frequency, phase, and pulse modulations. It is an advanced instrument which can

perform various functions in very simple and easy steps and provides better results to user demands.

Table 4.1: List of equipment used for channel measurement.

Equipment	**Usage**
Rohde& Schwarz SMBV100A	Vector Signal Generator
Rohde & Schwarz FSV7	Signal and Spectrum Analyzer
Rohde & Schwarz FSV7 B-22 Option	Preamplifier
Mini Circuits LZY-1+	50 W RF Amplifier
SpectraCom EC1S GPS Clock Reference	GPS Synchronization Device
RFS Dipole Antenna	145 MHz Antenna
A Custom designed Portable Radio Antenna	145 MHz Antenna
Different types of cables and connectors	Making connections

Rohde & Schwarz FSV7 signal and spectrum analyzer is used as a RX which offers a 160 MHz signal analysis bandwidth, a wide range of analysis packages for analog modulation methods, and supports wireless and wideband communication standards. What is more, it provides optimized measurement routines which makes its faster and increases data-throughput.

The maximum output power of SMBV100A signal generator is 30 dBm which is not enough to use for channel sounding in our measurement due to distance between transmitter and receiver that extend about 15 km. Therefore, 50W power amplifier's input is connected to the SMBV100A equipment's RF output in order to increase strength of transmitter output, in the output of PA power of signal can reach approximately 50W (≈ 47 dBm). This helps to withstand pernicious influence of channel as path loss and fading effects. Here, SMBV100A acts as master device output of which is connected to the PAs input and its output is connected to the 145 MHz dipole antenna. The generated signal is propagated around through the antenna. And received data is saved in the signal analyzer FSV7 which is employed as a receiver and a custom designed Portable Radio Antenna is used as its antenna. To strengthen the signal at the receiver side, the preamplifier option is used which is loaded into the device. It increases sensitivity of receiver by lowering the noise level, e.g. the FSV7 device's sensitivity to the noise is -155 dBm without preamplifier

measurements held in 1 Hz, and within preamplifier it is -165 dBm. As the receiver bandwidth increases the FSV7 device's sensitivity to the noise is also increases, e.g. when bandwidth of the devise is set to 24 kHz sensitivity of devise is -105 dBm, and when bandwidth is 2 MHz sensitivity is -90 dBm. The reason of giving the FSV7 devise's sensitivity at this bandwidth as an example is the measurement that we have done was held at this bandwidths.

The spectrum, I/Q (In-phase / Quadrature) vectors, and Constellation Diagram of received signal can be found by installed options in FSV7 device. In the desired frequency and bandwidth the signal can be obtained and displayed to users in various forms. Since the received signal is a complex RF baseband phenomenon,

$$y(t) = I(t) + j * Q(t), \;\; 0 \leq t \leq \infty. \tag{4.1}$$

measurements of the received signal I and Q sampling data should be obtained for channel impulse response (CIR). It can be done by using equation (3.1). In our work, the IQWizard program provided by Rohde-Schwarz Company is used to get I and Q data in wanted sampling frequency and bandwidth. Acquired I and Q data are recorded as MATLAB files to the computer and used in calculation of channel impulse response.

In order to perform channel modeling measurement frequency, phase and time of transmitter and receiver are required to be synchronized. Since the distance between transmitter and receiver is far in the current measurement, synchronization via cable is impossible. As a solution, signal generator and signal analyzer are set as slave devices, GPS satellites are selected as a master device, their trigger and reference signal are connected in channel measurement system. Therefore, GPS clock reference is needed to achieve synchronization between devices in time and frequency. For this purpose, SpectraCom EC1S GPS Clock Reference is implemented which produce 10 MHz reference signal and 1 PPS (one pulse per second) signal from received GPS antennas [14], [24]. These signals are connected to devices REF IN and TRIG inputs, respectively. The generator SMBV100A transmits signal when the device is triggered by the 1 PPS signal from TRIG inputs, and at the same time signal analyzer FSV7 starts to sampling when TRIG gets the trigger signal. As a result, both devices start to transmit and measure simultaneously. For the reason that GPS devices are locked to the same satellite at the same time, they

produce the same signals with very low margin of error. In this way the frequency, phase, and time synchronization problem can be solved.

4.2. Signal Design

In order to obtain channel impulse response, it is required to transmit probing pulse sequences through the channel, and received signal is recorded for some period of time than correlated with the original pulses, in that way impulse sequence is recovered. By adding pulses in this impulse sequence the signal-to-noise ratio (SNR) is increased and channel impulse response is obtained [25]. This method is shown in Figure 4.2.

Large scale fading is described by average path loss and shadowing, which relates the transmitted and received powers assuming no TX and RX loss or gain. So, for better SNR the bandwidth of the receiver should be adjusted properly, as the noise spreads out over all frequencies, it is obvious that if the bandwidth of the receiver is narrower the noise level is lower. Accordingly, for estimating large scale parameters bandwidth of the receiver is set to 24 kHz. Impulses sent in the method as mentioned above should have high amplitude. Otherwise, signal remains below the noise level. But this time it increases peak-to-average power ratio (PAPR). Considering 50 W amplifier that is used, it brings more harm to TX and environment. As a solution, the strength of impulses can be spread out in time domain, with that reducing the PAPR. To accomplish this, signal in frequency domain should be spread smoothly over channel bandwidth.

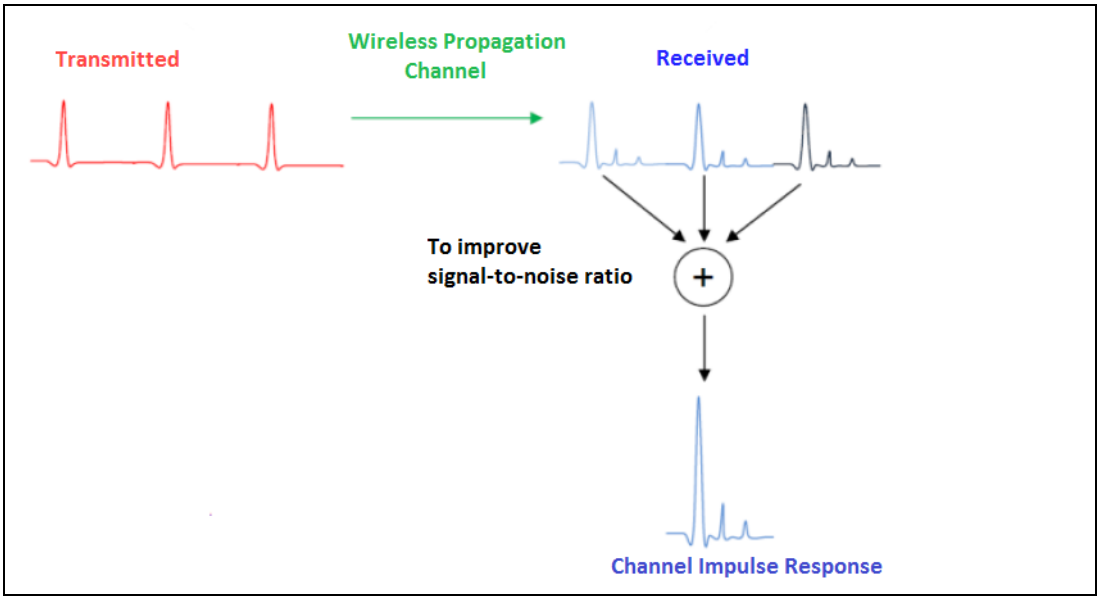

Figure 4.2: Impulse sequence method for signal design.

If the Fourier Decomposition method is applied to the signal in a frequency domain, it creates discrete frequency tones which uniformly spread over channel. By adding random phases to these tones spreading of the signal strength in the time can be realized. Then, by taking inverse Fast Fourier Transform (FFT) state of the signal in time domain can be propagated by transmitter. In this way, PARP is decreased but the strength of the signal is kept. In the receiver side inverse process is employed to obtain impulses, and by using them channel impulse response is computed.

The period of the signal in the measurement is set to 5.3 ms and channel is sounded in the continuous time which is 10 sec. The waveform that is used in measurement is generated in MATLAB environment and via the Ethernet cable transferred to the SMBV100A signal generator's Arbitrary Waveform Generator (ARB) units, graphs of the signal in the time and frequency domain are shown in Figure 4.3.

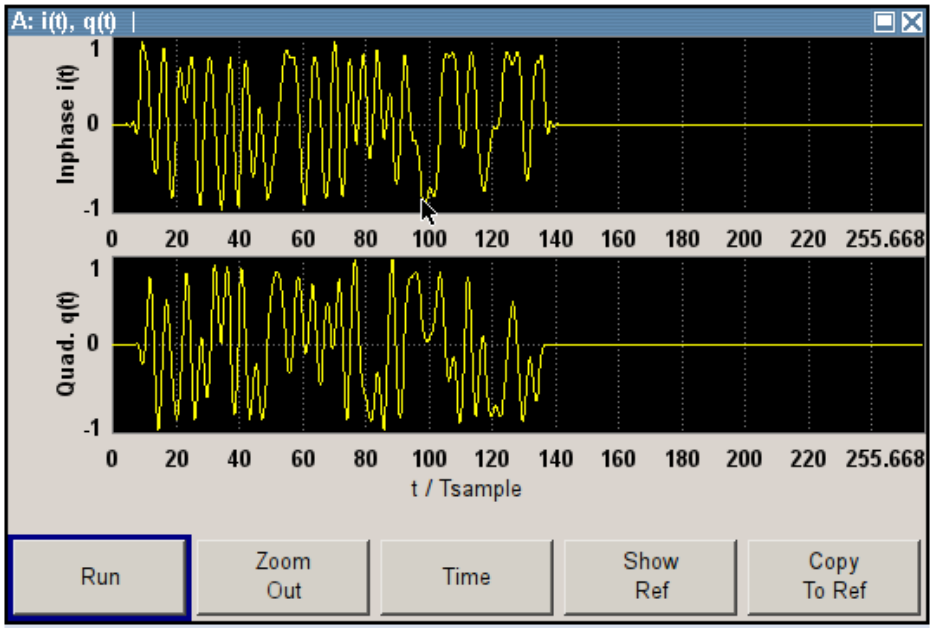

a)

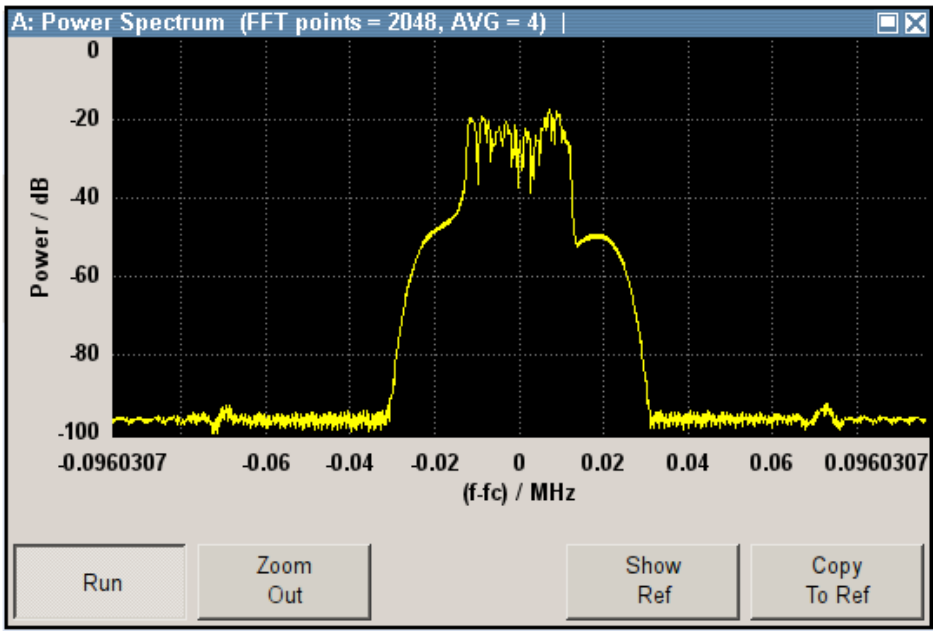

b)

Figure 4.3: Signal generated in the SMBV100A for large scale fading measurement a) I and Q components and b) Spectrum.

For the small scale fading analysis bandwidth of the receiver is set to 2 MHz which is much wider than used in measurement of large scale parameter (24 kHz). It was done in order to not miss multipath components of received signal. When channel measurement is carried out using pulse sequence method and data is used to analysis small scale fading following conditions must be taken into attention [1]:

- If period of the pulse smaller than the channel delay spread. Received impulses overlap with one another and become irresolvable in the correlation stage. To overcome this challenge sending period of signal must be greater than the channel delay spread.
- Duration of the impulse collection (the signal recording time on the receiving side) must be started and finished within the channel coherence time. For the reason that, if the channel changes while measurement is taken, received channel impulse response will not provide the real property of the channel.

In order to generate pulse sequences delay spread and channel coherence time values of 145 MHz frequency that belongs to VHF band must be known. The channel delay spread at VHF band in hilly, irregular terrain is reported to be smaller than 5 us. Channel coherent time of such channel at VHF band reported to be more than 10 ms [26]. The period of the signal in the measurement of channel is set to 104 us, where the pulse width is set to 4 us and channel is sounded for 1 second according to above information. Graphs of the signal in the time and frequency domain are shown in Figure 4.4.

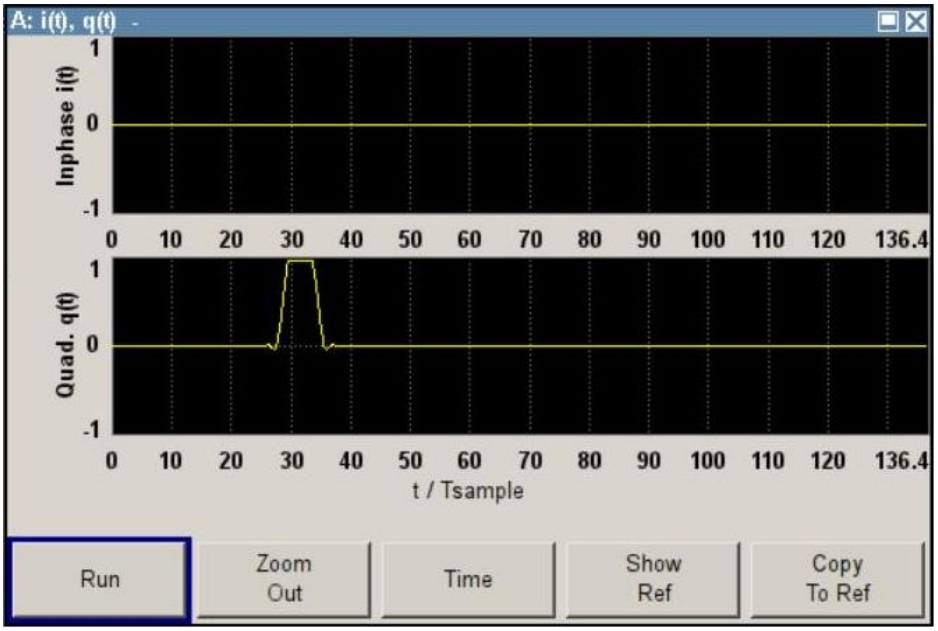

a)

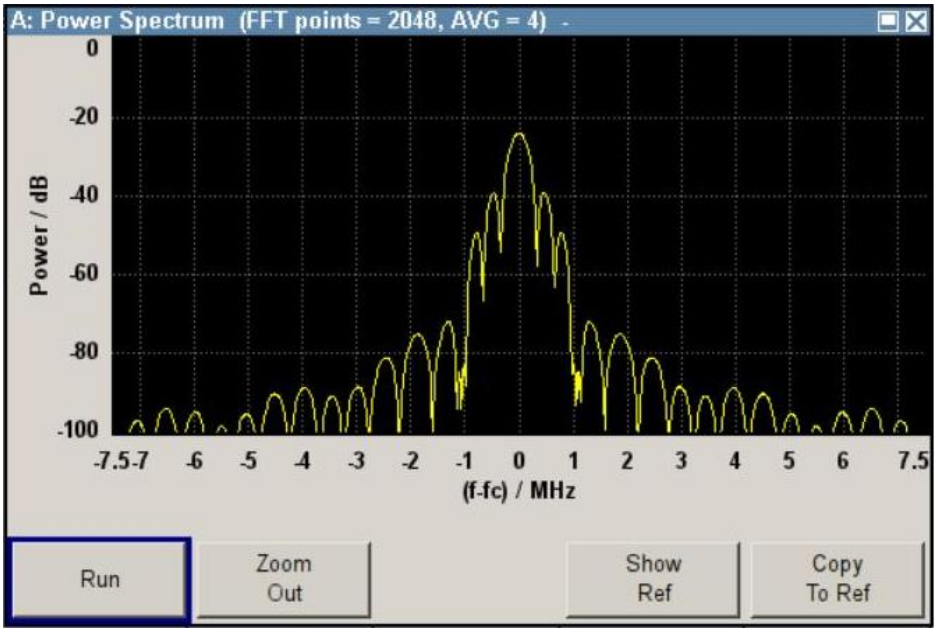

b)

Figure 4.4: Signal generated in the SMBV100A for small scale fading measurement a) I and Q components and b) Spectrum.

4.3. Link Budget Analysis

Calculation of all gains and losses in the transmission system, and examination of the receiver system elements that determines arriving signal strength is called link budget analysis. Link-budget analysis according to devices used in measurement, channel information and data available on previous works is shown in Tables 4.2.

This link-budget analysis show received power strength in dBm of the signal that is transmitted from 10 km far with a carrier frequency 145 MHz by output power strength 47 dBm. Here, SMBV100A signal generator is used as the TX and FSV7 signal analyzer is used as the RX. Signal strength that is obtained at receiver side depends on distance between TX and RX, antenna gains, path loss, losses in connecting elements and amplifier used in transmitter device.

The important point that must be considered in calculation of path loss is loss exponent value which must be selected according to environment where measurement is taken. In general path loss exponent varies between 2 and 4. The path loss exponent is 2 when free path loss is presented and 4 when too much scattering occurs [27]. In above analysis it is chosen as 3.5, the reason is our measurement take place in hilly irregular terrain where path loss intensity is high.

When path loss exponent is chosen 3.5, path loss expected to be approximately -167 dB. In this case for distance 10 km received signal strength is near -112 dBm.

Table 4.2: Link budget analysis.

System Variables	**Variable**	**Units**	**Equation**	**Value**
Frequency	f_0	MHz		145
Speed of Light	c	m/s		299792458
Wavelength	λ	m	$\lambda = c/f_0$	2.067534193

Table 4.2: Link budget analysis (continue).

System Variables	Variable	Units	Equation	Value
PA Power	P_{PA}	dBm		47
PA Power	Ppa	Watts		50.11872336
TX Match Loss	L_{MatchT}	dB		0
TX source	P_{TX}	dBm	$P_{TX} = P_{PA} + L_{MatchT}$	47
TX connector loss	L_{ConT1}	dB		1
TX cable loss	L_{CabT}	dB		1
TX feed loss	L_{ConT2}	dB		1
TX power	P_T	dBm	$P_T = P_{TX}$(C&C Loss)	44
TX antenna gain	G_T	dBi		2.1
Effective (Isotropic) Radiated Power	EIRP	dBm	$EIRP = P_T G_T$	46.1
Distance	d	m		10000
Path Loss	L_{FS}	dB	$L_{PLS} = 10\log(\lambda/4\pi d)^{\wedge}3.5$	-167.4315007
Power at RX Antenna, Hilly Environment	P_{ChanFS}	dB	$P_{ChanFS} = L_{PLS}$ EIRP	-121.3315007
RX antenna gain	G_R	dBi		2.1
RX connector loss	L_{ConR1}	dB		1
RX cable loss	L_{CabR}	dB		1
RX feed loss	L_{ConR2}	dB		1
RX Preamplifier	Ppre	dB		10
RX power	P_{RFS}	dBm	$P_{RFS} = P_{ChanFS} G_R$(C&C Loss)	-112.2315007

4.4. Data Collection

The real measurement is taken in Beypazarı-Ankara İnözü valley. Collected data are used to obtain needed results for channel modelling. The SMB100A signal generator and the transmitter antenna are located in the region's highest peak and by the FSV7 signal analyzer with the receiver antenna mounted on the vehicle measurement of the I and Q signals are taken along the valley with the interval 500 m between the receivers. Figure 4.5 illustrates the measurement view from the satellite. The height profile of the measurement points are the same as in ray-tracing based propagation channel modeling which is shown in Figure 3.2. And the line-of-sight distance between transmitter and receiver antennas can be found in Table 3.2 in 3rd chapter.

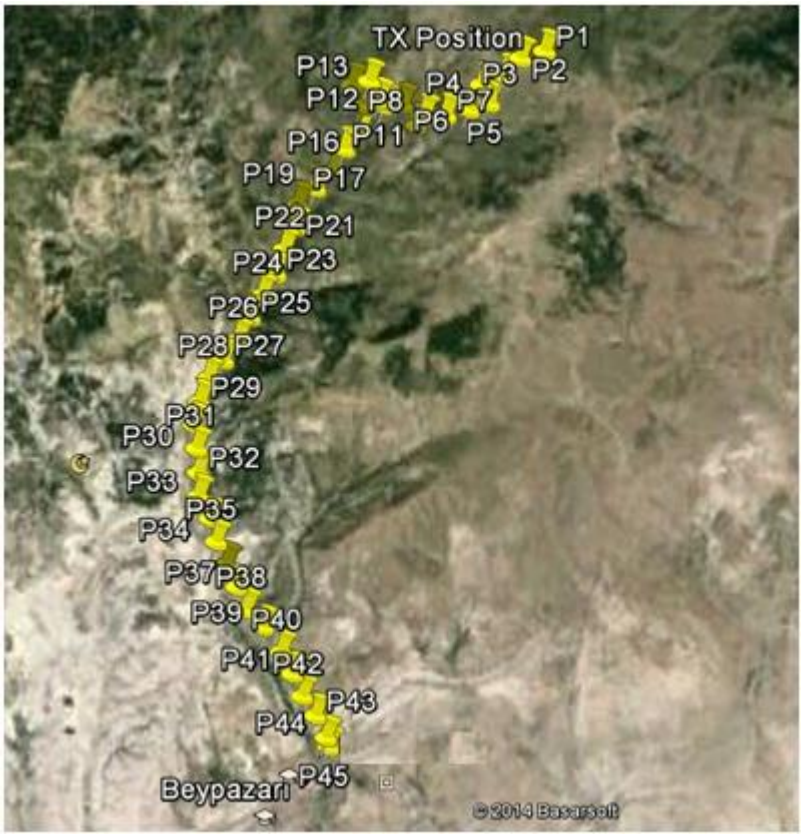

Figure 4.5: Data collection points on the measurement region.

5. MEASUREMENT RESULTS AND DISCUSSION

For both to ray-tracing based and empirical based channel propagation measurements the following statistics are obtained. Afterwords, these results are compared.

- Large scale statistics
  - Path loss:
  - Path loss exponent (n),
  - Shadowing parameter (σ),

- Small scale characteristics:
  - Power Delay Profile,
  - Time–Delay Spread,
  - First Arrival Delay,
  - Maximum Excess Delay,
  - Mean Excess Delay,
  - Root–Mean–Square (RMS) Delay Spread,
  - Coherence Bandwidth

are found. After, simulation and empirical results are compared.

5.1. Large Scale Fading Statistics

Obtained 45 I and Q data is used to calculate received power strength in the RX for each location points. Received power strength is found in terms of dBm by using equations (5.1) and (5.2):

$$IQ = |I + 1i * Q| \tag{5.1}$$

$$P_r = 30 + \log\left(E\left|\frac{IQ^2}{50}\right|\right) \tag{5.2}$$

where, 50 in the denominator of the absolute value in equation (5.2) come from 50 ohm receiver impedance.

Obtained empirical and WI received power data points are used in the interpolation of received power curves. In Figure 5.1 is shown empirical, WI and interpolation curve that represented by polynomial $1.1e\text{-}10*x^3+3e\text{-}06*x^2-0.028*x-18$. From this figure it can be seen that as the distance between TX and RX increases, as expected, received power decreases. It can be seen better in WI's output visually represented within modeled environment. Figure 5.2 illustrates received power in WI. For visual representation of the dependence the propagated signal strength from the environment illustration of signal path in WI is given in Figure 5.3.

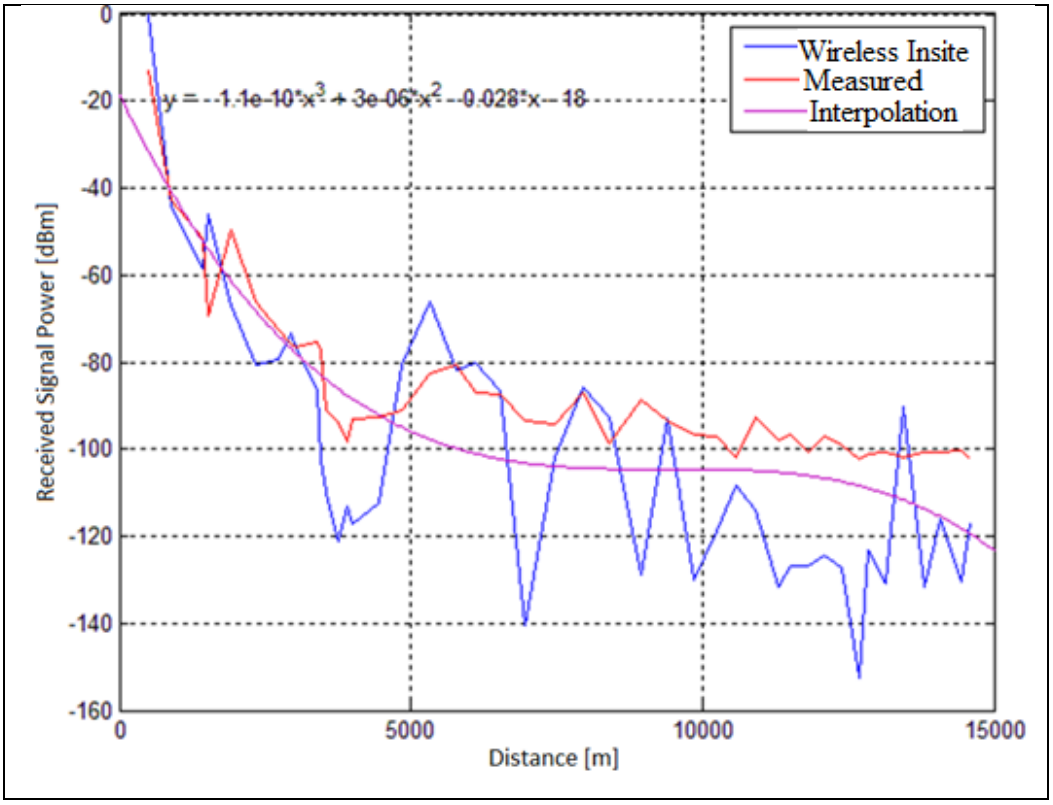

Figure 5.1: Received signal power vs. distance.

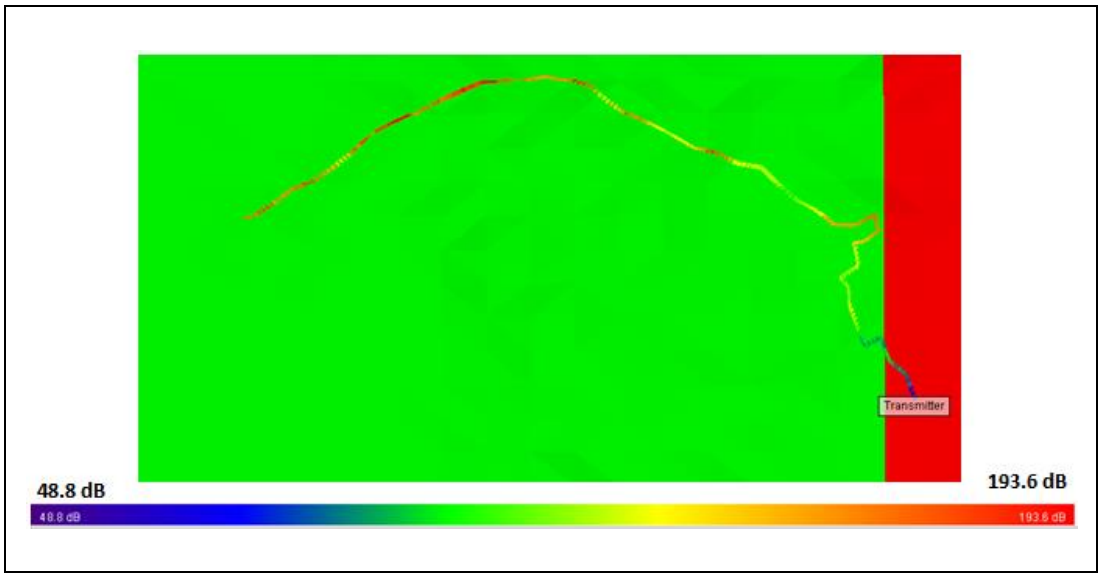

Figure 5.2: Received power visually represented within modeled environment – WI.

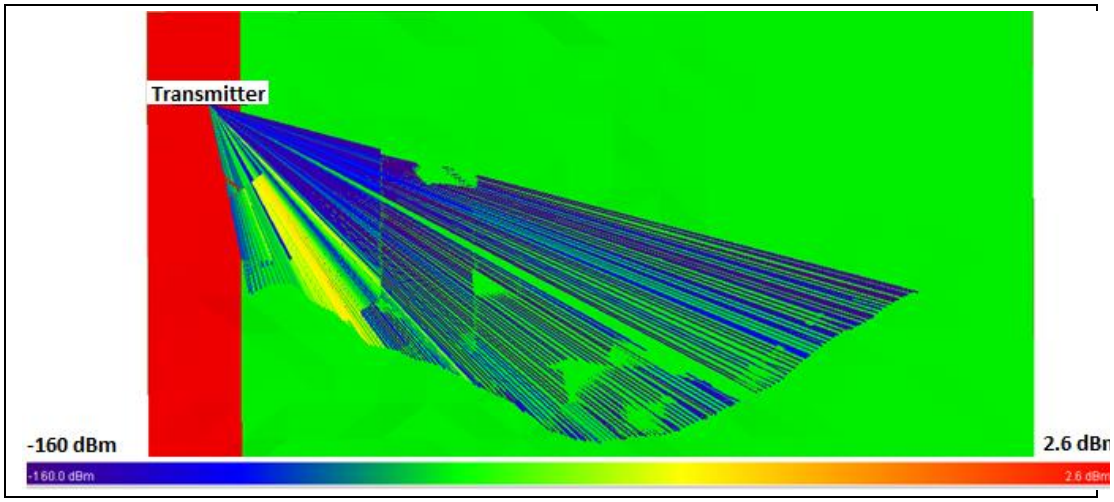

Figure 5.3: Propagation paths visually represented within modeled environment –WI.

From Figure 5.3 it can be seen that some paths are shadowed by higher hills, and the power strength reduction can be expected.

In order to estimate path loss exponent (n) and shadowing parameter (σ) the received power at a distance d from the transmitter must be calculated by using the following formula (5.3):

$$P'_r(d) = P_r(d_0) - 10nlog\left(\frac{d}{d_0}\right) \tag{5.3}$$

where, $P'_r(d)$ is received signal strength for a certain transmitter and receiver separation distance, P_r (d_0) is received signal strength at a close-in-reference-distance, d is certain TX and RX separation distance in meters, d_0 is the close-in reference distance from TX in meters which must be located in a far-field, the far field begins at a distance of 2λ and beyond. In our case it is chosen 40 m, our signal length λ is equal to 2,06753413 m.

Then, the minimum mean square error (MMSE) estimation is applied by using the formula (5.4) for estimating the path loss exponent (n):

$$J(n) = \sum_{i=1}^{k} \left(\left(P_r(d) - P'_r(d) \right) \right)^2 \tag{5.4}$$

where, P_r is the computed value, P'_r is the calculated value.

The next step was to equalize $J(n) = 0$ and compute path loss exponent (n) value, than using this result find shadowing parameter (σ) by using equation (5.5).

$$\sigma = \left(\frac{J(n)}{45} \right)^2 \tag{5.5}$$

After applying above methods to the received data from the measurement setup, empirical results are found. Empirical and WI results of path loss exponent and shadowing parameter are given in Table 5.1.

Table 5.1: Empirical and WI result of path loss exponent (n) and shadowing parameter (σ).

Path loss	**Empirical**	**Wireless InSite**
Exponent (n)	3.5138	3.7813
Shadowing parameter (σ)	6.2520	18.5241

As shown in the Table 5.1 path loss exponent parameter results in empirical calculation and WI are slightly different, and shadowing parameters have significant

difference. After, path loss in each point was computed by calculating difference between transmitted and received power in dBm. Used transmitted power was 50W (47dBm). Assuming cables and connectors losses P_T is calculated to be 45 dBm. For such situation path loss for each point is calculated by equation (5.6):

$$P_l = P_T - P_r \tag{5.6}$$

For real environments, the average received signal between the transmitter and receiver decreases with the distance in a logarithmic manner. The log-distance path loss model is given by the formula (4.7):

$$PL_{LD}(d) = PL_F(d_0) + 10nlog\left(\frac{d}{d_0}\right) \tag{4.7}$$

where, PL_F (d_0) is path loss in a free space, transmitter and receiver separated by distance d_0. This model can be constructed by modifying the free-space path loss with the path loss exponent *n* that is varies according to environment.

In Figure 5.4, it can be seen measured, WI, and log-distance *n*=3.5138 for empirical and n=3.7813 for WI based path loss curves. As it is shown in the graph, both empirical and WI path losses almost repeat each other with a difference in amplitudes. It is because of the difference in shadowing parameter (σ) and path loss exponent n.

The log-normal shadowing model's formula is given by equation (5.8):

$$PL(d)[dB] = \overline{\mathrm{PL(d)}} + X_\sigma = \mathrm{PL_F(d_0)} + 10\mathrm{nlog}\left(\frac{\mathrm{d}}{\mathrm{d_0}}\right) + X_\sigma \tag{5.8}$$

where, X_σ is a Gaussian random variable with a zero mean and a standard deviation of σ. This path loss model helps to construct the random shadowing effected by X_σ for the different shadowing parameter σ for receiver at the same distance d.

Figure 5.4: Path loss.

5.2. Small Scale Fading Statistics

Small-scale fading refers to the varying strength of wireless signals within a local area due to multiple signal paths which cause constructive and destructive interference when they arrive subsequently in the receive antenna with varying phase and time. This variation of the received signal occurs due to reflection and diffraction of nearby scattering surfaces. Additionally, each of the multiple signal paths may be changed by mobility of station and surrounding objects. Characteristics of a multipath fading channel are often defined by a power delay profile (PDP). The average power at the channel output as a function of the time delay (τ) is obtained by the power delay profile (PDP) and it is used to model small scale channel fading. It is calculated by measuring the spatial average of $|h(t, \tau)|^2$ over local area, where $|h(t, \tau)|$ is the channel impulse response (CIR) which is given by formula (5.9) that is represented by a discrete number of impulses as

$$|\mathrm{h}(\mathrm{t},\tau)|^2=\sum_{k=0}^{N-1} a_k^2\,\delta(\tau-\tau_k) \tag{5.9}$$

The power delay profile at the time t_0 for a probing pulse p(t) at the channel input is given by equation (5.10)

$$P(\tau_0) = |r(t_0)|^2 = \sum_{k=0}^{N-1} a_k^2\,(t_0) \tag{5.10}$$

Obtained 45 I and Q data from the measurement is used to find small scale parameters. First of all, CIR for the each point was found in volts and then the PDP in dBm was computed and plotted. Figure 5.5 gives an example for a) empirical and b) WI PDP of some points. From the graphs it can be seen that as the distance between the TX and the RX increase the received signal's time delay also slightly increase. It is because of,

$$d = c * t \tag{5.10}$$

where, *d* is distance separating transmitter and receiver, *c* is speed of light (signal propagated in wireless channel with the speed of light ~$3*10^8$m/s), *t* is the time when signal is received. It also can be seen from Figure 5.5, 5.6 and 5.7 that while the range between TX and RX increases there is a reduction in the signal strength.

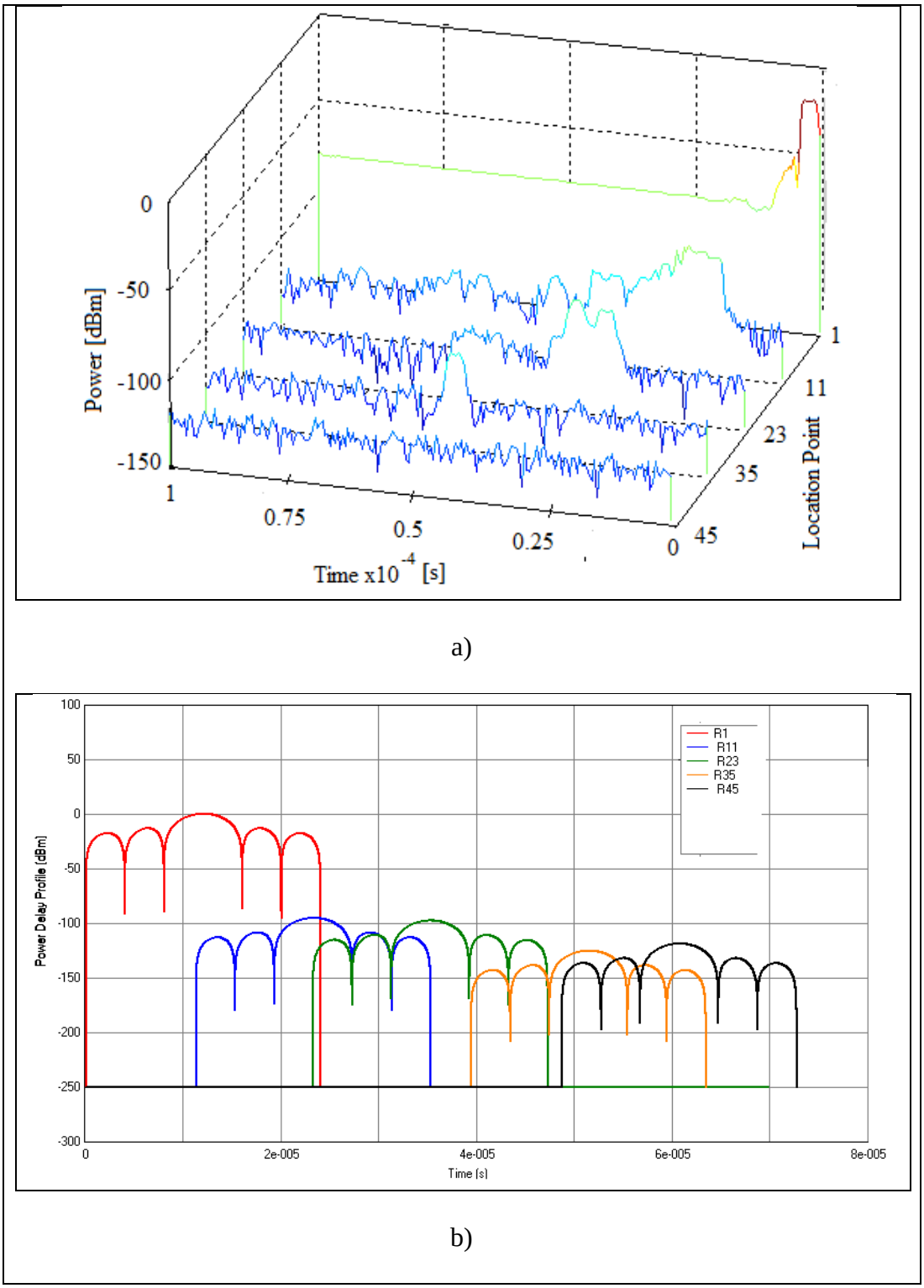

Figure 5.5: Power Delay Profile a) empirical; b) WI

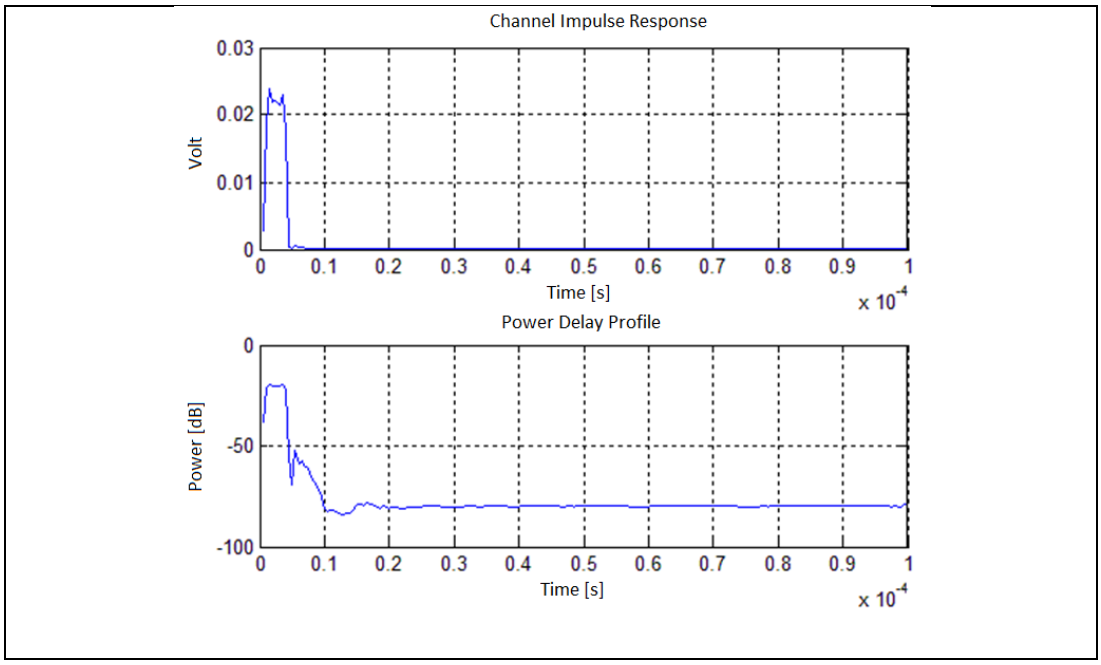

Figure 5.6: Channel Impulse Response and Power Delay Profile – Location Point 1.

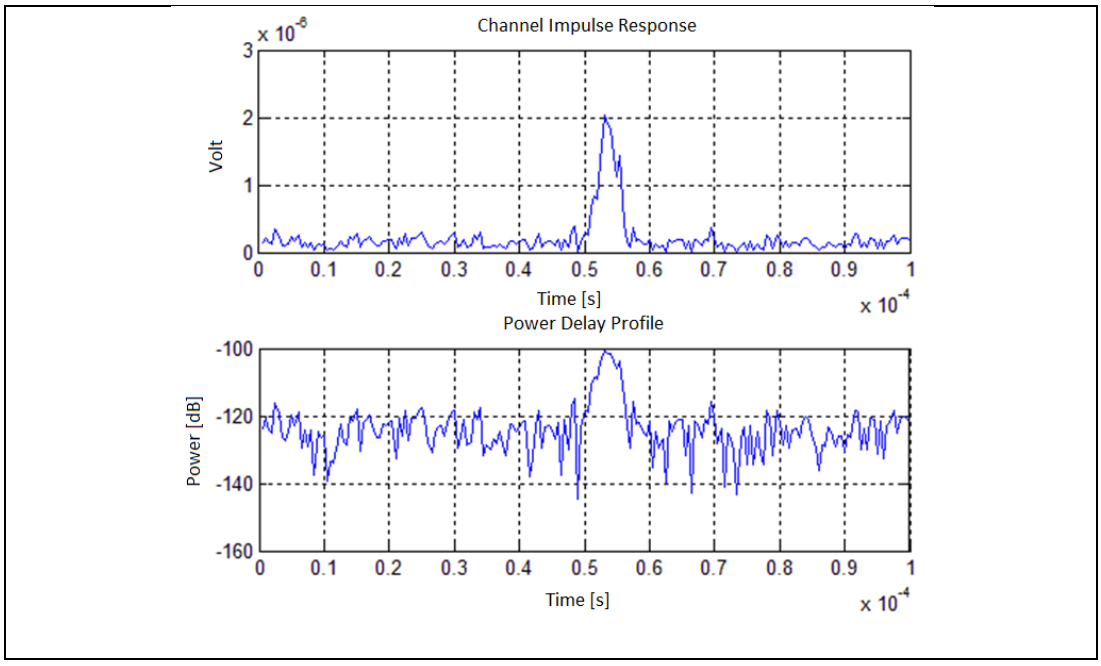

Figure 5.7: Channel Impulse Response and Power Delay Profile – Location Point 37.

Small scale fading channel statistics for real measurement are found by using decorrelation method and without eliminating correlation.

Decorrelation method has been applied to the obtained CIR [28]. If each sample of PDP assumed to be random variable, then PDP include 200 random variables. For each random variable, 9614 observation is available. If columns

assumed to be random variable and rows - observation, the measurement matrix with dimension 9614x200 can be obtained. The purpose of decorrelation process is to uncorrelate random variables by reducing correlation between them. In other words, observation matrix needed to be transformed to have a diagonal covariance matrix. This operation can be performed by the following steps.

If the observation matrix is X, then its covariance matrix can be found by equation (5.11):

$$\sum = Cov(X) = E[XX^T] \tag{5.11}$$

Obtained $\sum$ covariance matrix can be written in terms of eigenvalues and eigenvectors as shown in equation (5.12).

$$\sum = EDE^{-1} \tag{5.12}$$

where, *E* is a 200x200 matrix and each row indicates an eigenvector a corresponding eigenvalues. *D* refers to the eigenvalues of the covariance matrix. D is a diagonal matrix and can be expressed by equation (5.13).

$$E^T \sum E = D \tag{5.13}$$

Since $E^{-1}=E^T$, the above expression can be written in the form (5.13). By using matrix X, a new Y matrix with a diagonal covariance can be obtained by equation (5.14).

$$Y = E^T X \tag{5.14}$$

The results obtained by applying these processes and results without eliminating correlation are given below.

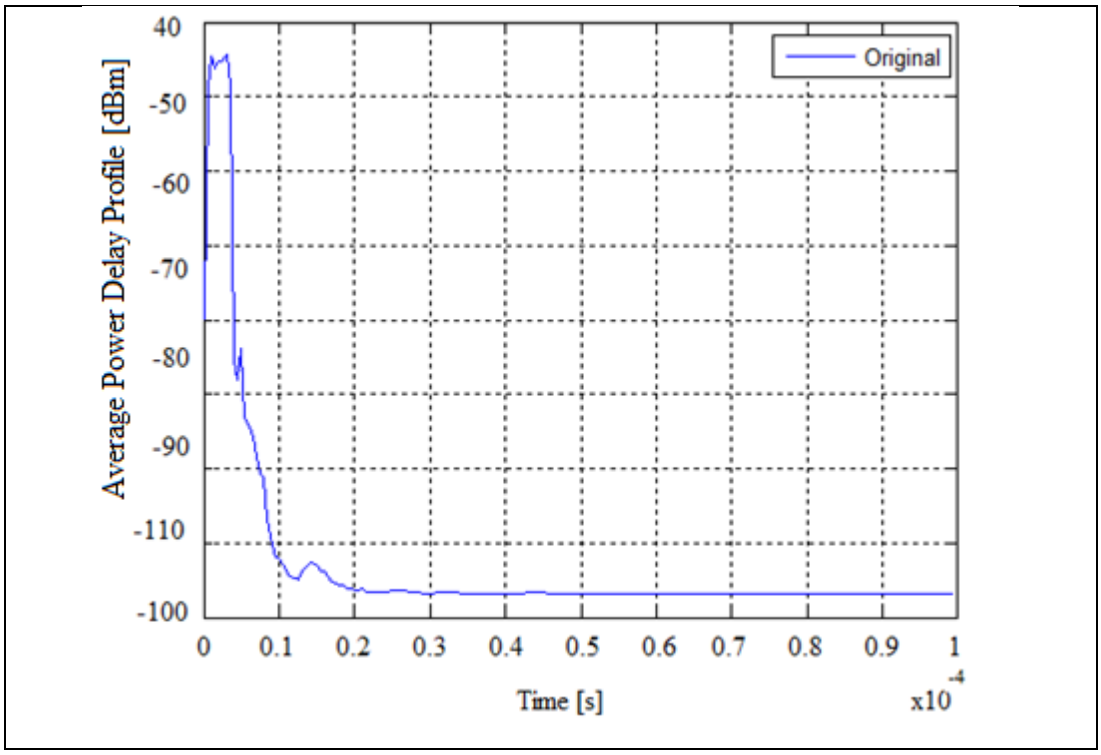

Figure 5.8: Average Power Delay Profile without eliminating correlation – Empirical.

As seen in Figures5.8 and 5.9, from decorrelated PDP received power of the multipath components can be distinguished clearly than the original PDP. In order to differentiate between multipath components and the noise, the noise threshold was chosen as -81.6681 dBm. After PDP is obtained, small scale characteristics are found according to decorrelated and without elimination of correlation PDP.

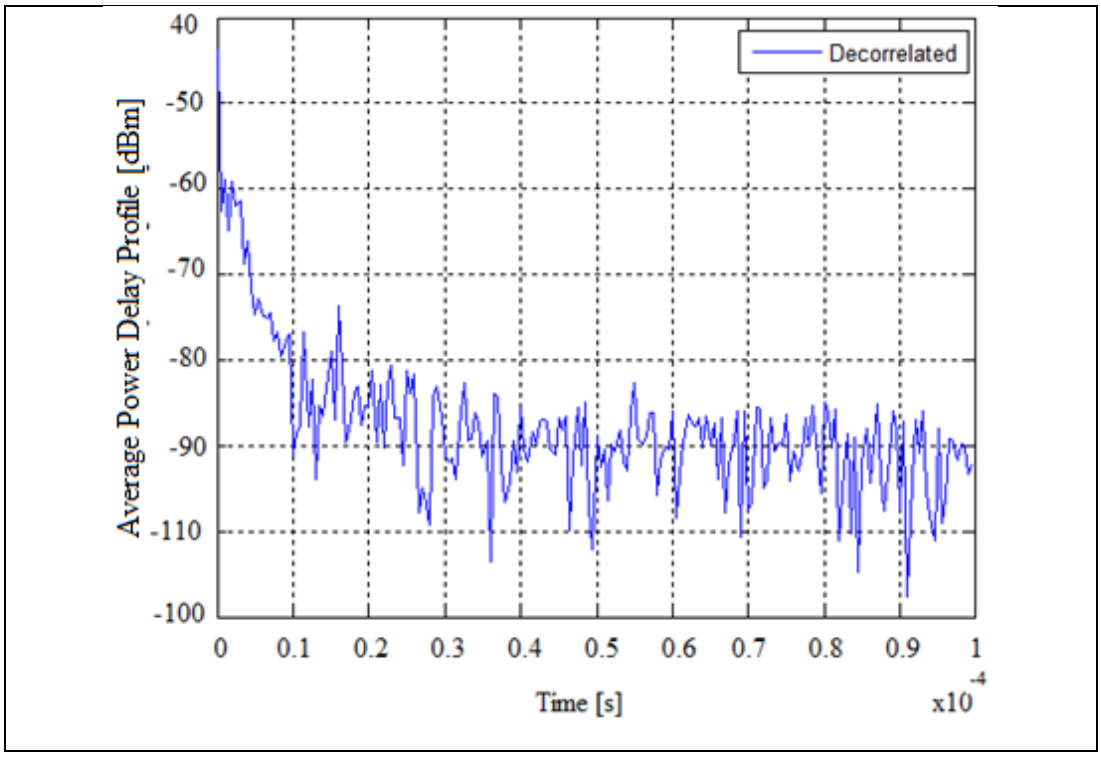

Figure 5.9: Decorrelated Average Power Delay Profile – Empirical.

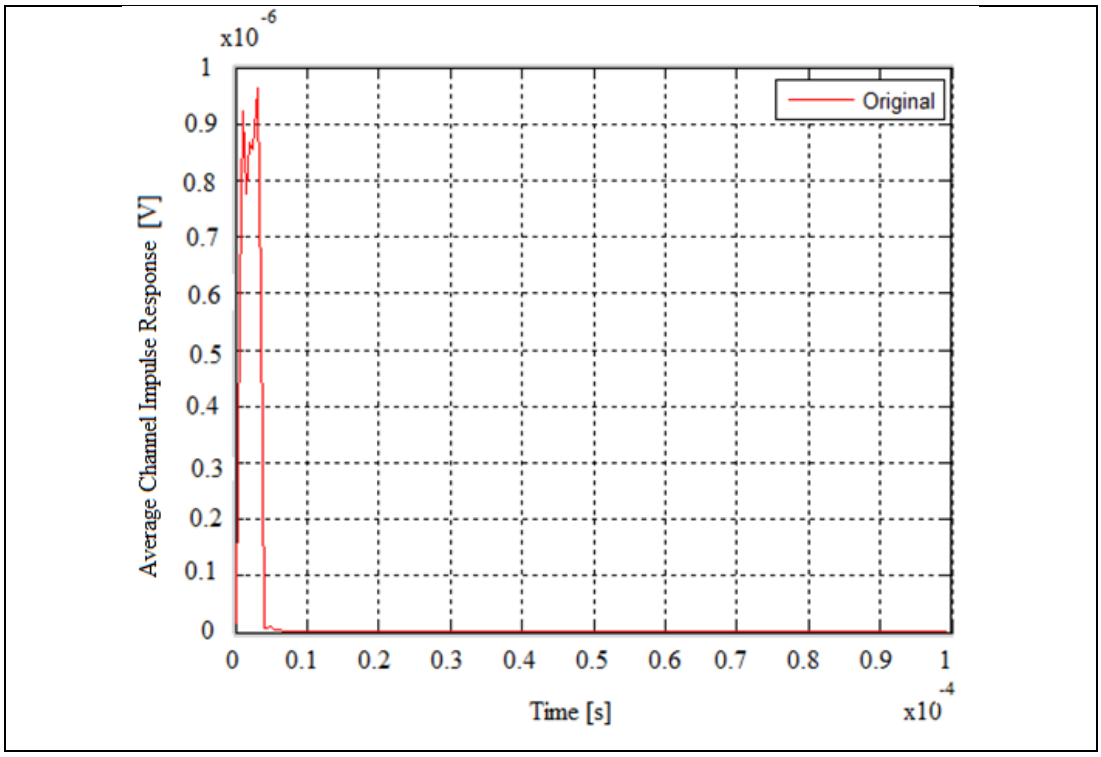

Figure 5.10: Average Channel Impulse Response without eliminating correlation – Empirical.

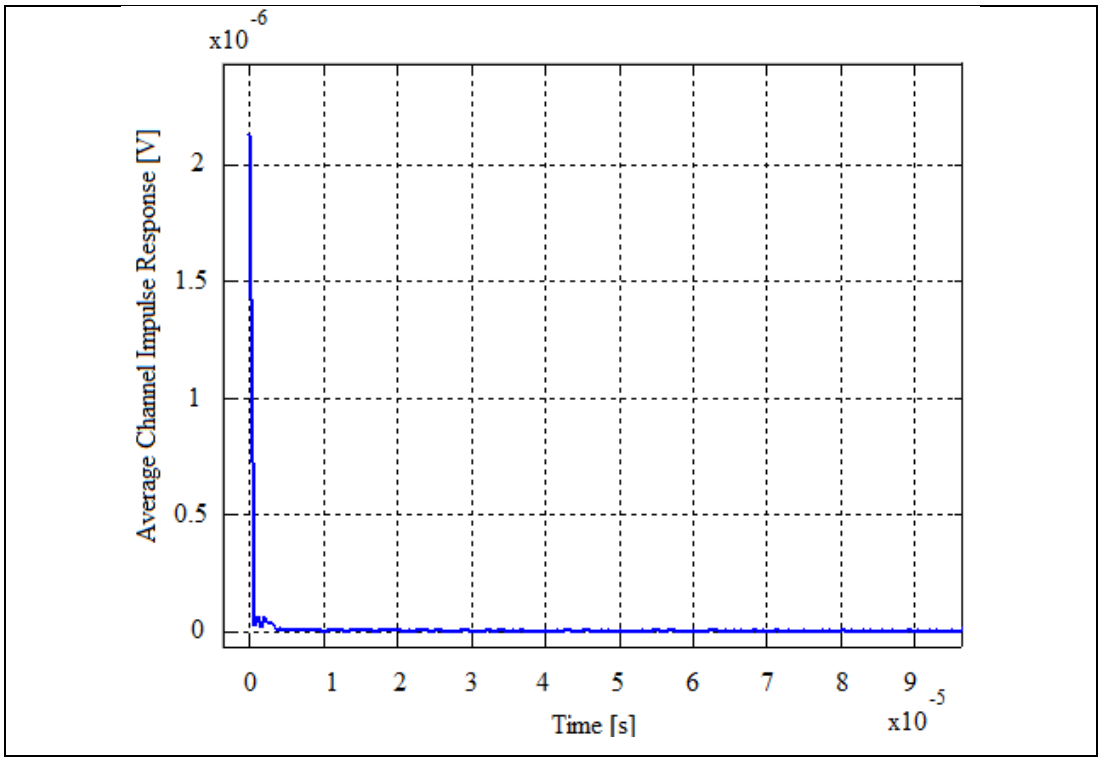

Figure 5.11: Decorrelated Average Channel Impulse Response– Empirical.

The first arrival delay of delay profile is defined to be the first arriving signal above the noise threshold.

The maximum excess delay of delay profile is defined to be the time delay during that multipath energy falls below the noise threshold and can be shown as

$$t_x - t_0 \tag{5.15}$$

where, t_0 is the first arriving delay of the signal and t_x is the maximum delay at which a multipath component is above the noise threshold.

The mean excess delay is the first moment of the power delay profile and is defined by formula (5.16):

$$\bar{\tau} = \frac{\sum_k a_k^2 \tau_k}{\sum_k a_k^2} = \frac{\sum_k P(\tau_k)\tau_k}{\sum_k P(\tau_k)} \tag{5.16}$$

The root mean square delay spread is the square root of the second central moment of the power delay profile and is defined by formula (5.17):

$$\sigma_\tau = \sqrt{\overline{\tau^2} - \overline{(\tau)}^2} \tag{5.17}$$

where, τ^2 is given by formula (5.18):

$$\overline{\tau^2} = \frac{\sum_k a_k^2 \tau_k^2}{\sum_k a_k^2} = \frac{\sum_k \tau_k^2 P(\tau_k)}{\sum_k P(\tau_k)} \tag{5.18}$$

The coherence bandwidth is used to characterize the channel in the frequency domain, Bc, which is inversely-proportional to the RMS delay spread. And it is the range of frequency domain the channel is expected to be unchanged and can be found by formula (5.19):

$$B_c \approx \frac{1}{\sigma_\tau} \tag{5.19}$$

Channel small scale fading statistics by decorrelation and correlation and results of Wireless InSite program are as following.

Table5.2: Comparison of empirical and Wireless InSite program small scale fading statistics' results.

Parameter	**Decorrelated**	**Correlated**	**Wireless InSite**
Maximum delay	26 us	44.6 us	44.3 us
Mean excess delay	2.48 us	9.53 us	12.9 us
RMS delay spread	3.26 us	3.43 us	2.32 us
Coherence Bandwidth	306 KHz	292 KHz	429 KHz

It can be seen from graphs of the channel transfer function in Figures 5.12 and 5.13 and from the table above that coherent bandwidth values are same and prove the correctness of each other.

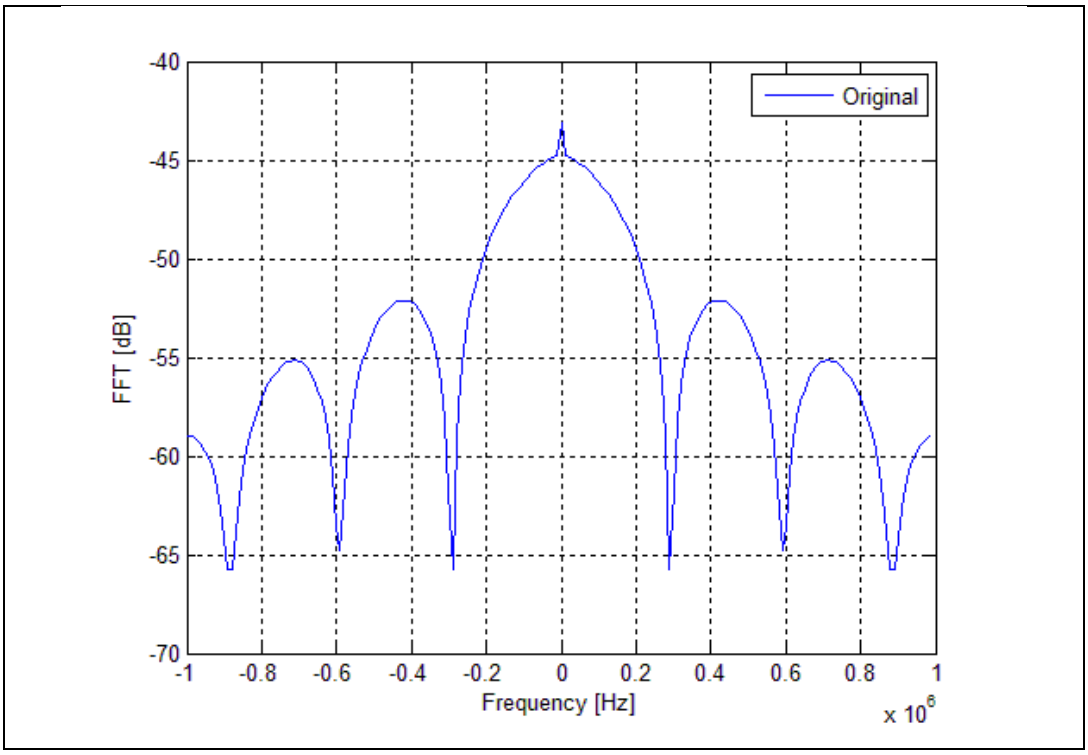

Figure 5.12: Channel transfer function of original signal.

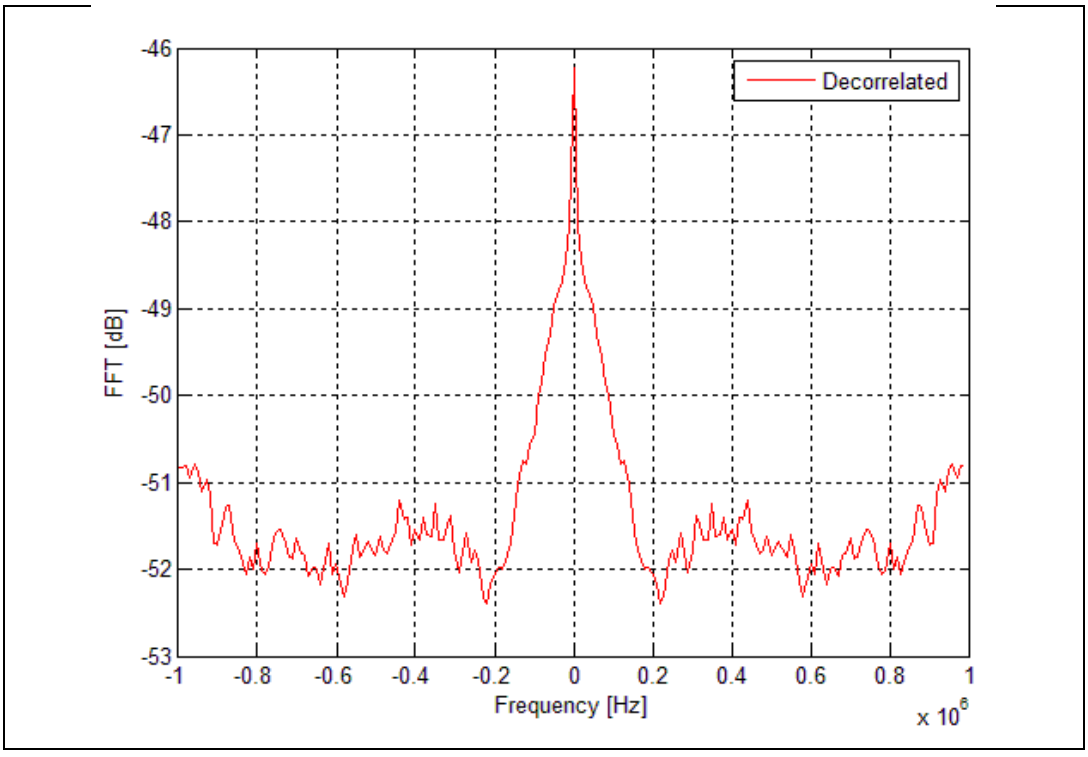

Figure 5.13: Channel transfer function of decorrelated signal.

6. CONCLUSION

In this thesis, empirical and ray tracing based propagation channel at 145 MHz Very High Frequency (VHF) communication band for wireless sensor networks is modeled. Simulation and empirical measurements are carried out in hilly and irregular terrain in Beypazarı-Ankara İnözü valley. The measurements are conducted at 45 different location points in the same environment for both real and ray-tracing based channel measurements by moving the RX while keeping the TX at a fixed location.

An electromagnetic simulation tool, the Wireless Insite software, is used to predict the propagation of waves through a wireless channel. The GIS data of Beypazarı-Ankara İnözü valley is imported and system parameters are set for ray-tracing based channel modeling, and analytical small scale and large scale fading parameters are obtained.

The data obtained from the measurements is used to estimate large scale fading parameters as path loss exponent and shadowing parameter. Additionally, it is used to generate power delay profiles and calculate the small scale parameters as maximum delay, mean excess delay, rms delay spread, and coherence bandwidth. These small scale parameters are calculated once again by using decorrelation method. Decorrelation is used to uncorrelate random variables of CIR by reducing correlation between them.

Based on the results obtained from ray tracing and measurements, a quantitative and a graphical comparison of channel statistics are done. From the comparison it can be seen the difference in results for empirical and simulations measurements. It is shown that by applying decorrelation method to the empirical channel impulse response rms delay spread and coherence bandwidth values come closer to the ray tracing measured results, and deviation between decorrelated empirical measurement and WI simulation measurement's rms delay spread and coherence bandwidth are 0.94 us and123 KHz, respectively. Additionally, when decorrelated method is applied to empirically obtained CIR, maximum delay decreases to 26 us from 44.6 us and mean excess delay decreases to 2.48 us from 9.53 us, deviation between decorrelated empirical measurement and WI simulation became 18.3 us and 10.42 us, respectively. These changes can be explained by the

fact that each multipath component in PDP became distinguishable by reducing correlation between random variables of CIR. The comparison of the large scale channel statistics show that results of path loss exponent n and shadowing parameter σ of ray tracing simulation are 0.2675 and 12.2721 dBm larger than empirical measurement, respectively.

This difference can be explained by ray tracing propagation algorithms that is used in software. The multipath propagation prediction of the waves through the channel is calculated based on Maxwell's equations in ray tracing simulation. Since Maxwell's equations are quite complex, algorithm that is used in ray tracing propagation makes high frequency approximations and considers the wave fronts to be plane waves.

The channel characteristics that are obtained in this work can be used in modeling the profile that can help to develop communication system for monitoring applications such as border security, surveillance of petrol/gas pipes or critical infrastructure/field in hilly and irregular regions.

REFERENCES

[1] MolischA.F., (2011), "Wireless Communications", 2nd Edition, A John Wiley and Sons Ltd.

[2] Michelson D.G., Ghassemzadeh S.S., (2009), "Measurement and Modeling of Wireless Channels". In: Vahid Tarokh, Editors, "New Directions in Wireless Communications Research", Springer Science+Business Media.

[3] Pasons J. D., (2000), "The mobile radio propagation channel", 2nd Edition, John Wiley and Sons Ltd.

[4] Cho Y.S., Kim J., Yang W.Y., Kang C.G., (2010), "MIMO-OFDM wireless communications with MATLAB", 1st Edition, Wiley and Sons Ltd.

[5] Fontan F.P., Espineira P.M., (2008), "Modeling the Wireless Propagation Channel A Simulation Approach with MATLAB", Wiley Series on Wireless Communications and Mobile Computing.

[6] Iftikhar W., Raichl J., (2008), "Channel Sounding", Master's Thesis, Halmstad University.

[7] Pedersen T., (2009), "Contributions in Radio Channel Sounding, Modeling, and Estimation", Doctor of Philosophy Thesis, Aalborg University.

[8] Zogg A., (1987), "Multipath Delay Spread in a Hilly Region at 210 MHz", IEEE Transactions On Vehicular Technology, 36(4), 184–187.

[9] Remcom Inc., (2012), "Wireless InSite Reference Manual", Remcom Inc.

[10] Remcom Inc., (2012), "Wireless InSite User's Guide", Remcom Inc.

[11] Web 1, (2015), https://www.rohde-schwarz.com/en/manual/r-s-smbv100a-vector-signal-generator-operating-manual-manuals-gb1_78701-37699.html, (Accessdate: 11/01/2015).

[12] Web 2, (2015), https://www.rohde-schwarz.com/en/product/fsv-productstartpage_63493-10098.html, (Accessdate: 11/01/2015).

[13] Meeks M.L., (1983), "VHF Propagation over Hilly, Forested Terrain", IEEE Transactions On Antennas And Propagation, 31(3), 483-489.

[14] Berger G.L., Safer H., (1997), "Channel Sounder For The Tactical Vhf-Range", MILCOM 97 Proceedings, 1474–1478, Monterey, CA, 02-05 November.

[15] Meng Y.S., Lee Y.H., Ng B.C., (2010), "Path loss modeling for near-ground VHF radio-wave propagation through forests with tree-canopy reflection

effect", Progress In Electromagnetics Research, 57(5), 1461–1468.

[16] Swarts F., Ferreira H.C, (1991), "A Comparison Between Stationary And Mobile Digital Vhf Radio Channels And Channel Models", Communications and Signal Processing, COMSIG 1991 Proceedings, South African Symposium, 74–79, Pretoria, 30 August.

[17] Pugh J.A., Bultitude R.J.C., VigneronP.J., (2007), "Propagation Measurements and Modelling for Multiband Communications on Tactical VHF Channels", Military Communications Conference, 1–7, 29-31 October.

[18] Dias M.H.C., Rotava A., Andrade F.G., Alem R.A., Melo M.A.K., Santos J.C.A., (2011), "Path Loss Measurements of HF/VHF Land Links in a Brazilian Atlantic Rainforest Urban Site", IEEE Antennas And Wireless Propagation Letters, 10, 1063–1067.

[19] Li H.J., Chen C.C., Liu T.Y., Lin H.C., (2000), "Applicability of Ray-Tracing Technique for the Prediction of Outdoor Characteristics", IEEE Trans. Veh. Tech., 49(6), 2336–2349.

[20] McKown J. W., Hamilton R. L., (1991.), "Ray tracing as a design tool for radio networks," IEEE Network, 5(6), 27-30.

[21] Zhao X., KivinenJ., Vainikainen P., Skog K., (2002), "Propagation Characteristics for Wideband Outdoor Mobile Communications at 5.3 GHz," IEEE Journ. Selected Areas Comm., 20(3), 507-514.

[22] Domazetovic A., Greenstein L. J., Mandayam N.B., Seskar I., (2005), "Propagation Models for Short-Range Wireless Channels With Predictable Path Geometries," IEEE Trans. Comm., 53(7), 1123 - 1126.

[23] Web 3, (2015), http://data.geocomm.com/catalog/TU/group121.html (Accessdate: 25/06/2015).

[24] Hu C., Zhou Z., Guo S., (2013), "Synchronous Wideband Frequency-Domain Method For Long-Distance Channel Measurement", Progress In Electromagnetics Research, 137, 643–652.

[25] R&SGmbH & Co. KG., (2013), "Channel Sounding in White Space Spectrum. Customer Application Note", Rohde & Schwarz GmbH & Co. KG.

[26] Web 4, (2015), http://www.ece.vt.edu/swe/lwa/memo/lwa0134.pdf (Accessdate: 1/05/2015).

[27] Andersen J.B., Rappaport T., YoshidaS., (1995), "Propagation Measurements and Models for Wireless Communications Channels", IEEE Communications Magazine, 33(1), 42-49.

[28] Dony R.D., (2001), “Karhunen- Loeve Transform”. In: Rao K. R., Yip P.C.. Boca Raton Editors, “The Transformand Data Compression Hand book”, CRC Press LLC.

BIOGRAPHY

Aizat Aitalieva was born in Talas, Kyrgyzstan, in 1988. She received the B.Sc. degree in electronics engineering from International Ataturk Alatoo University, Bishkek, Kyrgyzstan, in 2012. She started her M.Sc. degree at Gebze Technical University Graduate School of Natural and Applied Science Electronics Engineering Department in 2012 and received the M.Sc. degree in electronic engineering in 2015.